

3 Phase Atrous Net with DCO-3DSPMRINET Model for Scoliosis Prediction

Spurthi Adibatti^{1*}, K. R. Sudhindra², Joshi Manisha S³

Submitted: 18/10/2022

Revised: 14/12/2022

Accepted: 29/12/2022

Abstract: Intervertebral Disc (ID) is the mattress like structure that holds the bones of the spine together thus these discs increase the stability of the spinal column and ID images are used in the prediction of Scoliosis disease. However, while processing these images existing techniques use edge operators to locate four points on vertebral body for prediction of disc bulge but it is very difficult to obtain such image because the severity in the selected plane image is still uncertain. Hence a novel Quadruple Up Sampling Operation up sample the images double times with the Omnidirectional sagittal block matching algorithm that select, match and label the image hence, the intervertebral disc's severity and the plane image as a slice of the present frame remain predictable. Moreover, during segmentation it is impossible for 3D structure to reconstruct automatically due to over segmentation and it provide only less detail about disease growing rate. Hence the technique 3 phase Atrous Net automatically segment and predict the sub image pair by segmentation and elastic atlas mapping with the cascade and parallel atrous convolution thus provide separation between vertebral disc near together and overcome over segmentation with the Duck colony optimization algorithm for feature selection. However, in classification stage semantic and discreet reconstruction limit the detail in image feature extraction so it results in perplexing outcome. Hence 3DSpMRINET technique uses sparse learning that provide feature weight vector that enhances the quality of the image and provide a high accuracy of disease classification. The proposed model for scoliosis prediction has been implemented in python platform and the result shows improved accuracy, recall rate, precision and F1 score.

Keywords: Intervertebral disc, scoliotic, quadruple up sampling operation, 3 phase atrous net, 3DSpMRINET, accuracy, omnidirectional sagittal block matching algorithm.

1. Introduction

The biomechanical system of human body is made up of vertebral bodies (vbs) and intervertebral discs (ivds) [1]. Back pain, caused by conditions such as spondylolisthesis and spinal stenosis, is the most prevalent reason for adult clinical visits in modern cultures, resulting in substantial costs and impairing life quality and work performance [2]. Pathological lesions, fractures, tumors, degeneration, protrusion, or herniation of the vbs or ivds can all cause spinal problems. As a result, robust segmentation methods must be used to analyze their form, position, orientation, and tissue etiology for diagnosis and preoperative/therapy planning [3]. Noninvasive noncontrast enhanced magnetic resonance (mr) imaging gives improved contrasts for tissue segmentation. Manual segmentation is time-consuming, expensive, and prone to errors, but well-designed automation algorithms may provide dependable, robust segmentations for research with a big cohort or over a lengthy period of time Recently proposed methods for automatically segmenting vbs/ivds [4,5] on mr images used

a local or global/local model of the vbs/ivds' shapes, geometries, pairwise geometric constraints, and intensities to initialize and steer their registrations/deformations towards object boundaries [6], avoiding convergence to local extrema and reducing computations [7]. If numerous vbs/ivds were to be segmented, this meant sequential localization/segmentation [8].

Besides computational complexity, one by-one localization of VBs/IVDs [9] could be confused by the repetitive pattern of the spine and similarities in intensities or shapes of neighboring VBs/IVDs. So far, these ambiguities were addressed by a spatial probabilistic map [10] obtained from a trained CNN model, a parzen window applied to the training images, or a hidden Markov model of relative shapes, poses, and distances of neighboring VBs/IVDs. In these methods, having significant shape, geometry, and intensity variations [11-13] in the training images could enhance the generalizability of the learnt segmentation model. However, they reduced the specificity of the resolved localizations [14]. Furthermore, most of the previous methods for segmenting VBs/IVDs relied on T1- or T2-weighted MR images. Chemical-shift encoded (Dixon) MR imaging provides high contrasts for a simultaneous assessment of morphological properties and fat content of spinal structures. Observed associations

^{1,2} Dept of Electronics and Communication Engineering BMSCE Bangalore,INDIA

³ Dept. of Medical Electronics BMSCE Bengalore, INDIA

between these measures and demographic state, bone mineral density, osteoporosis/osteopenia, degenerations, visceral obesity, and diabetes motivate further analysis via automated assessments on large cohort data sets [16]. So far, only a few methods have been developed based on fat-water MR images. These methods either performed a one-by-one localization/segmentation or used deep learning with high computational complexity [17].

Segmentation of intervertebral discs has similar difficulties, i.e., partial volume effects and gray-level overlapping, with one of the most researched segmentation tasks, the segmentation of brain tissue from MR images [18-19]. Soft segmentation techniques such as the fuzzy c-means algorithm (FCM) have been widely used for dealing with partial volume effects in brain segmentation [20]. The accurate segmentation of intervertebral discs would be useful in quantification of disc degeneration and computer-aided diagnosis of the disease as well as computer-assisted spine surgery [21-24]. So far, most studies dealing with the quantification of disc features for diagnostic or surgical purposes have been based on manually segmented data. However, manual segmentation is a tedious and time-consuming process where there is a lack of reproducibility between observers. However, none of these studies reported on the quantitative evaluation of segmentation accuracy. Moreover, the segmentation of degenerated intervertebral discs appears to remain an open issue therefore to overcome the discussed issue a novel model for analyzing the disc images with high segmentation accuracy is required. The main contribution of this paper are as follows,

- In scoliosis disease prediction from ID images, issue in predicting pre-defined plain image in preprocessing stage has been removed by using quadruple up sampling operation by performing the up sampling double times.
- In segmentation the automatic reconstruction of the 3D structure denied the detail about disease rate which is solved by 3 phase atrous net that automatically segment image with the duck colony optimization algorithm for the feature selection.
- In the prediction of severity of scoliosis disease there is the limit of detail in image for feature extraction which is solved by 3DSpMRINet which uses sparse learning for estimation of feature weight vector.

The content of the paper is structured as follows: section 2 denotes the literature survey, section 3 provides technique and the novel solution, results obtained are provided in section 4; finally, section 5 concludes the paper.

2. Literature Survey

Rehman et al [25] uses the probability map of a pre-trained deep network to initialize the level set and refines the

output repeatedly under the operation of multiple factors. As a result, the network's learning ability is increased, and the network can accept large topological form changes in the vertebrae. On two separate datasets, the proposed technique was tested. The first is a collection of 20 publicly accessible 3D spine MRI datasets for disc segmentation, while the second is a set of 173 computed tomography scans for segmenting thoracolumbar (thoracic and lumbar) vertebrae. U-Net architecture, on the other hand, fails to perform and obtain suitable segmentation performance when dealing with segmentation situations with substantial topological shape variability.

Hwang et al [26] proposed a radiomics model to distinguish hematopoietic marrow disorders and compared the results to radiologists' readings and a quantitative measurement. The images acquired from multiple manufacturers, models, magnetic fields, and scanning parameters were normalized with the annulus fibrosus of a non-degenerated intervertebral disk in order to minimize the effect of image heterogeneity on radiomics features. This may have added consistency among the images acquired from multiple manufacturers, models, magnetic fields, and scanning parameters. It was difficult to identify key characteristics to distinguish diseased marrows since LASSO, PCA, and RF chose various feature groups; nevertheless, the six radiomics models distinguished diseased marrows with high CA, SE, and AUC with little variation.

Fallah et al. [27] created an automated measurement of the morphological and fat-related characteristics of VBs and IVDs. This enables huge cohort data sets to be used in investigations on subclinical spinal diseases. It might also be used for other segmentation aims by changing its feature set to appropriate multimodal or multichannel images, such as T1-, T2-, and PD-weighted images, or Dixon data sets of other quantitative maps. Their thinness, on the one hand, made them vulnerable to noise or partial volume effects, and on the other, hinted that they had little impact on the segmented volumes.

Lin et al [28] described an object-specific bi-path network (OSBP-Net) for axial spine image quantification. The OSBP-Net has a shallow feature extraction layer (SFE) and a deep feature extraction sub-network for each route (DFE). Because the two target organs have distinct anatomical diameters, the SFEs employ various convolution strides. Based on the finding that the target organs have lower intensity than the background, the DFEs employ average pooling for down sampling. The DE-Net, on the other hand, is built for generic organ quantification, which means it doesn't take use of the inherent qualities of axial spine estimation, resulting in inferior predictions.

Pang et al [29] introduced SpineParseNet, a two-stage accurate and robust multi-class segmentation system, to do spine parsing. The suggested area pooling module, which

was constrained by the deep supervision loss, created a trustworthy graph representation, which was developed by consecutive graph convolutions. The region unpooling module projected the evolving semantic network representation to a semantic image representation. The IVDs, on the other hand, are difficult to see clearly on the CT picture.

Li et al [30] addresses the problem of fully-automatic localization and segmentation of 3D intervertebral discs (IVDs) from MR images. Our method contains two steps, where we first localize the center of each IVD, and then segment IVDs by classifying image pixels around each disc center as foreground (disc) or background. The disc localization is done by estimating the image displacements from a set of randomly sampled 3D image patches to the disc center. However, if the image does not contain all the 7 discs (T11-S1), then our algorithm may fail, because the location of the missing discs returned by our algorithm may be completely wrong.

Wang et al [31] identified patient presenting AIS thus the major curve apex on PA X-rays was chosen as the region of interest (ROI) for machine learning from 52 patients who had routine PA spinal X-rays. For the pre-training and fine-tuning of the model, a two-stage transfer learning technique was introduced. The major curve's apical rotation and torsion were shown to be considerably different between the P and NP curve trajectories using 3D reconstruction. Cross-platform performance on standard standing PA X-rays produced accuracy, sensitivity, and specificity values of 77.1%, 73.5%, and 81.0%, respectively. When the degree of apical rotation or torsion differed from that of the succeeding curve trajectory, errors in prediction occurred, but they could be fixed by taking serial X-rays into account. Performance was better than that of clinical parameter-based regression models and conventional CNNs. The need for pricey biplanar X-ray devices, then the labor-intensive and error-prone software reconstruction of each individual vertebra, continue to be impediments to deployment.

Nault et al [32] explain a prospective cohort of AIS patients had 3D reconstructions at their initial orthopedic visit was enrolled. Five different types of descriptor measurements were made: the angle of the maximum curved plane, Cobb angles, 3D wedging, rotation, and torsion. Final Cobb angle (either shortly prior to surgery or at skeletal maturity) was used as the outcome, while 3D spine characteristics and clinical data were used as predictors in a general linear model analysis with backward selection. The final model has a determination coefficient (R^2) of 0.643 and incorporates significant predictors such as beginning skeletal maturation, curve type, frontal Cobb angle, angle of plane of maximal curvature, and 3D disc wedging (T3-T4, T8-T9). The corresponding positive and negative predictive values for a 35-degree curve are 79%

and 94%, respectively. The model will assist the treating doctor in starting the right course of treatment on the initial visit. However, this investigation did not identify that apical vertebral body wedging as a predictor.

Zhang et al [33] proposed a two-phase study with an exploration group of 120 AIS and a validation cohort of 51 AIS with mean Cobb angles of 23° and 5.0° at the first visit each. In order to create a composite model for prediction, patients with AIS were tracked for a minimum of six years. Clinical parameters were gathered on the initial visit from standard clinical practice, and blood was tested for circulating markers. The composite model has a larger area under the curve than do the individual factors currently employed in clinical practice. The model had a sensitivity of 72.7% and a specificity of 90% after being validated by a separate cohort the initial study to propose and validate a prognostic composite model based on clinical and circulation characteristics that could objectively assess the likelihood that an AIS curve would proceed to a severe curvature. The study, however, did not provide information on the relationship between treatment outcome and disease severity.

Yi et al [34] proposed the innovative landmark detecting technique for the vertebrae. The model initially locates the vertebral centres; from there, it uses the learnt corner offset to trace the vertebra's four corner landmarks. This allows us to maintain the landmarks' original order when using our strategy. The comparison findings show the advantages of our method in landmark detection and Cobb angle measurement on ambiguous and low-contrast X-ray images. However, this technique suffers from the class imbalance issue between the positive and negative points since each channel in the output feature map has only one positive point, which will harm the model's performance.

For [25], it fails to perform and obtain suitable segmentation performance, for [26] it is difficult to identify key characteristics to distinguish diseased marrows. In [27] must improve thinness, on the one hand, made them vulnerable to noise or partial volume effects, for [28], need a right prediction thus it does not take use of the inherent qualities of axial spine estimation that resulting in inferior predictions, for [29], it is difficult to see disease clearly on the CT pictures, for [30], is completely wrong about the missing disc, for [31], it is impediments to deployment, for [32], it did not identify that apical vertebral body wedging as a predictor, for [33], it does not predict the disease severity, for [34], the performance of the model is class imbalance.

3. 3 Phase Atrous Net with DCO-3DSPMRINET Model for Scoliosis Prediction

In recent years, the scoliosis is found to be a tragic because of its wideness over the people it is a three-dimensional

deformity of the spine with a prevalence these is the disease more prominently found in the female category than the male which should be predicted in the initial stage to overcome the severe problems in the spinal intervertebral column. However, for processing ID images and their illnesses, existing models manually locate the spinal cords centre at each vertebral level using edge operators which in turn yields open contours for scoliotic patients as it is very difficult to obtain such image since the degree of severity in predefined plane image. Hence a novel model is proposed in the preprocessing stage named Quadruple Up Sampling Operation thus the images are up sampled double times and images are selected using a novel method known as Omnidirectional sagittal block matching algorithm thus the matching images are labelled that finds the best matches of current block in the current frame. Therefore, the degree of severity resulted as motion vectors and the plane image as a slice of given current frame inter vertebral disc remains predictable.

Moreover, Automatic reconstruction of 3-D structures is not possible when employing the watershed technique on gradient images during segmentation because this leads to over segmentation issues. Thus the distortion, inconsistencies, and lack of information on disease segmentation occur in the existing model. Thus a novel technique 3 phase Atrous Net that combines both segmentation and elastic atlas mapping provide the sub image pairs are mapped in registry as spatial information that incorporates locations, edges and shapes of ROI image structures that are delineated to obtain binary disc templates thereby overcoming Distortion and inconsistencies that occurs during reconstruction of the image thus the segmentation is done using atrous convolution in cascade and parallel way that provide minimal separation between vertebral disc near together thus overcome over segmentation. After performing feature extraction, the feature selection is done using Duck Colony optimization algorithm with respect to scoliosis disease the Cobb angles its intensity, height and density with respect to mathematical richness are selected as best features by considering these parameters.

Furthermore, due to the application of semantic reconstruction and discrete reconstruction, both of which limit the details in the image for feature extraction, this failed to produce a high-quality image at the retrieval stage. This led to the same patient being diagnosed with multiple conditions by using multiple weighted images, which also led to confusing results. Hence the Selected features by the various parameters of best features are then trained to 3DSpMRINet that uses sparse learning estimate a feature weight vector, which is compelled by a sparsity regularization term to contain many zeros and only have a few non-zero weights corresponding to the chosen features. Thus it improves the accuracy of the disease classification

and quality of image during retrieval process thus the severity of the scoliosis disease is predicted from the low, medium and high with the angle representation.

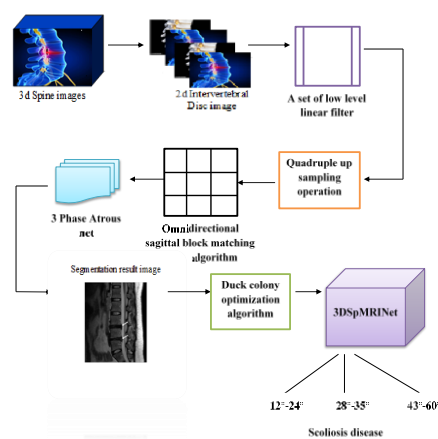


Fig. 1: Architecture of proposed Scoliosis disease prediction model

The proposed model for the scoliosis disease prediction is given in figure 1, in which the 3D image is converted into 2D image and then the set of linear level filter is used thus the preprocessing step get continued the input is sampled up double times by the up sampling operation the block matching algorithm matches the sample thus atrous net is combined with the segmentation and atlas mapping in which the resultant segmentation image is obtained therefore an duck colony optimization is used and 3DSpMRINet predict the scoliosis disease effectively.

3.1 Quadruple Up Sampling Operation

The segmentation in 3d spine dataset provided the unsupervised pictures thus 2d image of these images are then created and a set of low level linear image filters are used in preprocessing as it involves the proper selection of images for labelling and processing. In quadruple up sampling operation the image is up sampled double times up sampling manipulate a signal in order to increase the sampling rate which is the post processing tool that increases the resolution of the images. Quadruple up sampling consist of the up sampling of the 2D image that is more beneficiary due to its efficiency in increasing the spatial resolution of the image in greater extent with up sampling which also increase the size of the image. The goal of up sampling is to eliminate low level pixilation. The classification of the quadruple up sampling process is given in figure 2.

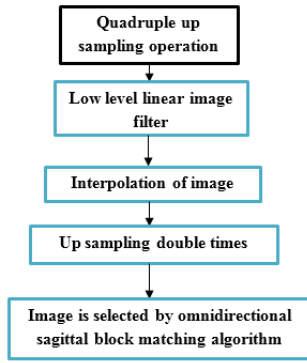


Fig. 2: Process in quadruple up sampling operation

In quadruple up sampling operation it works in the preprocessing stage in which the low level linear filter is used which filter the image for its processing then the interpolation of the image is carried out in the preprocessing step that provide the image resizing thus the remapping of the image is carried out by the interpolation process of image then the image is up sampled double times to enhance the resolution of the image thereby eliminating the low level pixelation of the image. The image is up sampled double times in which it repeats the rows and columns of the input and thus the sample get improved for its quality and performance. The interpolation of the image is explained in the equation (1),

$$f(p, q) = (1 - c)(1 - d)F(i, j) + (1 - c)dF(i, j + 1) + c(1 - d)F(i + 1, j) \quad (1)$$

Where, the image interpolates in p direction at first and then interpolate in q direction. To generalize cubic interpolation to two dimensions, a 44 sub grid with 16 samples is required here i and j are the row and column of sub grid thus c and d is represented as dimension of sub grid. The interpolation of the image is given by the matching images that labelled the current match. The up sampling of double times is caused to have the image with its specific characteristics. Thus the image is selected by the omnidirectional sagittal block matching algorithm. The disease is predicted by starting the search location on the affected area positive or negative S pixel is searched for its location thus the new search origin picks the location search procedure is carried out for obtaining the pixel to be 1. The symmetric measure for matching diseased region is estimated by the γ which is given in equation (2),

$$\gamma = \frac{|GFD_L - GFD_R|}{GFD_W} \quad (2)$$

The symmetric measure for disease region matching is found as the difference between Growth Finding Distance in left (GFD_L) and the growth finding distance in right (GFD_R) and the total degree of growth finding distance is GFD_W . The multifractal spectra values of the image is given by the ROI centered image of sagittal plane with the

prediction of ROI features p_i of the input intervertebral image is given in equation (3),

$$\mu_I(p, q) = \frac{p_i}{\sum_{i=1}^n p_i^p} \quad (3)$$

The difference in symmetric measure is determined by the maximum value of the symmetric measure of the intervertebral image and the minimum measure of intervertebral image is given in equation (4),

$$\Delta\gamma = \gamma_{\max} - \gamma_{\min} \quad (4)$$

Thus the output sub image pair S_0 is obtained with high multifractal spectra values and the symmetric measures in the omnidirectional sagittal block matching algorithm select the images and label the matching images accordingly. The omnidirectional sagittal block matching is explained in the algorithm as follows,

Algorithm 1: Omnidirectional sagittal block matching algorithm

Input: intervertebral image

Output: sub image pair

Initialize scoliosis prediction model

{

Start with search location centre

Search location +/- S pixels around location (0,0)

Set the new search origin to the above picked location

Repeat the search procedure until step size $S=1$

Exact the initial sagittal region from the image

Estimate the symmetric measure by equation (2)

Consider ROI centered on C^* and select sagittal plane S within the ROI centered image

Compute the $\mu_I(p, q)$ as for $i: 1 \rightarrow n$ using equation (3)

Determine the difference of symmetric measure of $\Delta\gamma$ using (4)

Find the S_0 based on $\Delta\gamma$ value from ROI of MRI plane

Obtained S_0, MSP

end

}

The omnidirectional sagittal block matching algorithm predict the input intervertebral image to analyze with the location centre which is searched for the disease location thus the process picked the location with the stepping size of 1 by removing the extreme region the of initial sagittal region thus the symmetric measure is estimated thus the

region of interest (ROI) is centered by the C* of the sagittal plane thus the MRI plane is computed and exhibit the sub image pair S_o and the Multi spectra prediction (MSP) denoted as from ROI by the multifractal spectra values in the magnetic resonance imaging plane of the image. The multi spectra value of the image is given by the value of $\mu_l(p, q)$ in the block matching algorithm.

3.2.3 Phase Atrous net

The 3 phase Atrous net combine segmentation and elastic atlas mapping thus in segmentation it is often based on the properties of the picture's pixels, image segmentation divide an image into various parts or areas. The sub image pairs are mapped in registry as spatial information using this three-phase Atrous Net, which incorporates the locations, edges, and shapes of ROI image structures that are delineated to obtain binary disc templates, thereby overcoming distortion and inconsistencies that occur during image reconstruction. Additionally, to capture multi-scale context and provide rich, complex features that accurately capture each patient's information, the segmentation is carried out using atrous convolution in cascade and parallel fashion. A large feature pool is created after completing feature extraction for each patient; it is composed of RGB color channel picture characteristics such as histogram representation, grey scale features, area features, sob features, and root sum mean square features. The segmentation in 3d spine dataset provided the unsupervised pictures thus 2d image of these images are then created and a set of low level linear image filters are used in preprocessing as it involves the proper selection of images for labelling and processing. In order to overcome the segmentation issues in the Intervertebral disc images. The image segmentation by the 3D phase atrous net is given in figure 3.

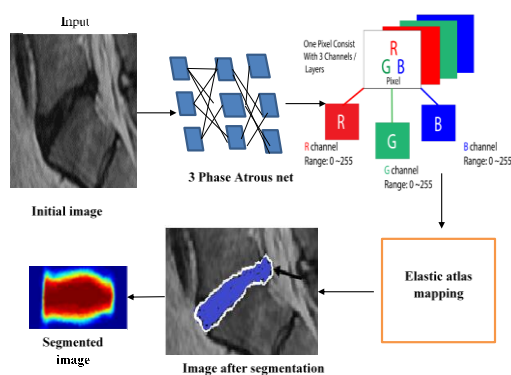


Fig. 3: Image segmentation by the 3 phase atrous network

Figure 3 explains the image segmentation by 3 phase atrous network. The 3 phase atrous network with the RGB color channel segment the image with the color for the prediction and the mapping of the diseased part which is labelled by the coloring partition in the image using the elastic atlas mapping in segmentation the disease is mapped correctly.

This elastic deformation method is based on a multiscale framework that captures both large- and small-scale transformations while taking into account regional variations in image brightness and contrast. It assumes a locally affine and globally smooth transformation in the segmentation of the image. The elastic atlas was initially aligned with the picture using a strict landmark-based registration procedure. The amount of the fuzziness of resulting classification is given by

$$F = \sum_{j=1}^w \sum_{k=1}^s \mu_{ik}^m \cdot \|y_i - v_k\|^2 \quad (5)$$

$$v_k = \frac{\sum_{j=1}^w \mu_{ik}^m y_i}{\sum_{j=1}^w \mu_{ik}^m} \quad (6)$$

where y_i is a pixel's intensity, s is the number of clusters or classes, w is the total number of pixels in the picture, ik is a pixel's membership in each class, and v_k is the value of the cluster centres for each class. Three membership matrices were created using the class membership values of each pixel. The registered atlas DPbest matrix were then multiplied pixel-by-pixel to create a combined probability matrix representing the disc image. By automatically thresholding this combined probability, the segmented disc was produced. Thus the feature selection is done by duck colony optimization algorithm in which the with respect to the scoliosis disease the cobb angles its intensity, height and density with respect to mathematical richness need to be selected thus the fitness function of the optimization algorithm is given in equation (7),

$$FitnessF = \max (f_{c1} + C) \quad (7)$$

Where f_{c1} is the cobb angle of the intervertebral image and C is the segmented input image thus the fitness value is the maximum of the segmented and the intervertebral image thus r_1 is the random variable selected before selecting best value of the feature the intervertebral disc with the number of cluster equal to 1 is given in equation (8),

$$DV(s = 1) = C1DV(s) + C2r_1(DPbest(s) - DPnd(s)) \quad (8)$$

The intervertebral disc image velocity is represented as DV thus $C1DV(s)$ represents the 1st segmented intervertebral disc image $DPbest(s)$ indicate the best value of the feature thus the intervertebral disc image as the segmented image input made the output with the feature selection. The end feature of the position vector of the image is obtained by the $DPnd$ with the additional cluster or group is given in equation (9),

$$DPnd(s + 1) = DPBest(s) - C1 \cdot |C2 \cdot DPbest(s) - DPnd(s)| \quad (9)$$

$$DPnd(s + 1) = DPnd(s) + DV(s + 1) \quad (10)$$

The position vector of the input segmented image is found out so that the feature selection is carried out by the optimization algorithm thus the speed of the feature selection process is further revised by using equation (11).

$$\Delta Ds + 1 = h\Delta Ds + C1r1 (DPebests - Ds) + C2r2 (DPGbests - Ds) \quad (11)$$

$$Ds + 1 = Ds + \Delta Ds + 1 \quad (12)$$

The speed of the feature selection process is given by the equation (11) thus this depicts the importance of the feature selection for its efficient speed. Equation (12) shows the location change by the optimization image. This algorithm specifically used for feature selection with respect to the cobb angle intensity, height and density. Thus the duck colony optimization algorithm is explained as follows.

Algorithm 2: Duck colony optimization algorithm

Input: Segmented image

Output: Feature selection

do

{

Initialize D_i features of intervertebral data

while the stop condition is not pleased

for each duck

Call segmented image to find the classification accuracy

if classification accuracy < DP-pbest

Travel with the present assessment to DP-pbestmatrix

end if

For each duck

Revise the groceries and predator **Revise** $fc1, C1, C2, r1, r2$,

Compute objective function fn for each duck DP_i

Revise neighboring radius R

if a duck has at least one adjacent duck

Revise velocity vector using equation (8)

Revise position vector using equation (9)

else

Revise position vector using equation (10)

end if

According to the changeable restrictions ensure and approved the original locations

end while

For each duck in a duck flock **Initialize** ducks with DP-pbestmatrix allocate DP-Pbest

end

While Nx_{is} is not attained

For each duck

Call segmented image to find the classification accuracy

if classification accuracy < DP-pbest in the past **Allocate** present assessment as the original DPbest(s)

end if

end for

Pick the duck with the best fitness value of duck flock in DT-Gbest

For each duck

Speed calculated using equation (11)

Location changed using equation (12)

end for

end while

$best\text{-fitness} = AC - DPbest(s)$ /*AC is atrous convolution */

end while

}

The Duck colony optimization algorithm initialize the intervertebral data in which the duck population $D_i, i = 1, 2, \dots, n$, maximum iteration Nx_{is} , $s = 0$, number of search ducks thus the velocity and position vector in the duck colony optimization algorithm provide a output for feature selection from the input intervertebral image based on cobb angle thus the prediction of the scoliosis is carried out by the feature selection in the image.

3.3 3DSpMRINet

The 3DSpMRINet uses the sparse learning to improve the disease classification accuracy. The scoliosis disease is predictable which is given by the 3 dimensional magnetic resonance imaging. The severity of the scoliosis condition was then divided into three categories such as low severity (Cobb 12–24), moderate severity (Cobb 28–35), and high severity (Cobb 43–60) thus the classification with greater accuracy is given by the cobb angle that is predicted with the accurate value. The Cobb angle is the primary determinant that determines the treatment approach that is ultimately adopted since the severe problem occurs due to the higher value of cobb angle. The sparse learning in the sense of the prediction of disease in the network. Thus the

sparsity reduces the representation complexity in every prediction range. The concept of sparse matrices is extended to include sparse networks in processing 3D MRI images. A *DPbest* matrix makes sense if there are few non-zero items in each row and column the non-zero elements and their positions in a unique data structure, significantly reduce memory needs and speed up operations. The spatial location to be active by the vector of a spatial position in the input layer graph is not zero, the place is deemed active. If any of the spatial locations in the layer below from which it receives input are active, then declare that any spatial location in a hidden layer is active. On those sparse vectors, data between layers is transformed using techniques like convolutions, pooling, and nonlinear activation functions. Data in regions with inactive voxels, which make up the majority of them, do not depend on a voxel's relative position, so smaller vectors without specified spatial dimensions is used in their place. The sparse learning is used here to estimate the feature weight vector of the segmented image the sparse net is less complicated structure than the other neural network which may provide the cobb angle of the disease area that exhibit the severity of the disease and the problems in the disease prediction process. The 3DSpMRINet for the disease prediction is given in the figure 4 below.

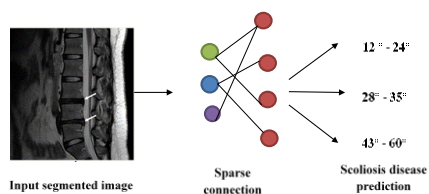


Fig. 4: Disease prediction by 3DSpMRINet

Figure 4 shows the scoliosis disease prediction by 3DSpMRINet in which the segmented image is given as the input to the sparse learning connection where the sparse connection is linear to produce non complicated structure of the sparse net thus the connection predicts the cobb angle of the disease and thus the scoliosis disease is predicted in a distinct manner. The predicted angles and the landmark are given by the equation (13) given below.

$$y^{\wedge}(t) = sDVK(t) \quad (13)$$

The equation (13) indicates the angle prediction of the model in which *s* is given by the multiple of the cluster or group of the image, *DV* indicate the disc image velocity thus the *K(t)* is the activation function used to divide it in three angles based on severity condition as low severity (Cobb 12–24), moderate severity (Cobb 28–35), and high severity (Cobb 43–60) for the prediction of the scoliosis disease.

Overall, the proposed model exhibits the prediction of the scoliosis disease by preprocessing the 3D image into 2D image and then up sampled for double times using the quadruple up sampling operation which predict the predefined data for the degree of severity prediction then the segmentation is done by the 3 phase atrous net that uses the elastic atrous mapping and duck colony optimization algorithm for feature selection and the 3DSpMRINet provide the cobb angle of the prediction of the severity of the disease and sparse learning is used for the feature weight estimation thus the high quality and accurate disease prediction model is obtained. Thus the accuracy of the disease prediction is increased by this method and the quality of the image also get increased by applying these technique thus the experimental output in the next section depict the output of the proposed method.

4 Results and Discussion

4.1 Experimental output

This work has been implemented in the working platform of python with the following system specification and the simulation results are discussed below.

Platform: Python

OS : Windows 10

Processor: 64-bit Intel processor

RAM : 8 GB RAM

4.2 Dataset description

Spine sag T2W dataset is used in this research to effectively predict the scoliosis disease and the 3D reconstruction of spinal structures, 3D automated segmentation (MR) pictures of multiclass spinal structures are required. It offers quantitative analysis tools for creating biomechanical models of the spine, modelling stresses in spinal structures, and evaluating the likelihood of success for various spinal degenerative disease treatments. With the help of artificial intelligence technology, this competition intends to bring together international developers to investigate effective and precise 3D automatic segmentation of spinal structure in MR images. There are ten vertebrae and nine intervertebral discs in the spinal system that has to be segmented.

4.3 Simulated output from proposed model

The scoliosis is predicted from the 3 phase Atrous net with the DCO-3DSPMRINET and number of objects using the novel techniques and the result obtained are discussed in this section.

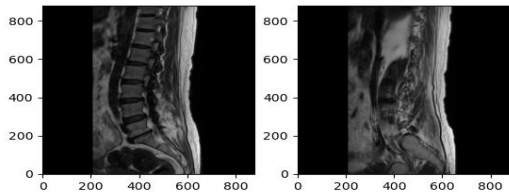


Fig. 5: Conversion of 3D image to 2D image

Figure 5 depicts the input image taken from the 3D image from the 3D spine image dataset and the conversion of 3D image to 2D image and the process involve in the conversion of the image is the important term in which they help in the prediction of the disease with the greater accuracy than the 3D image.

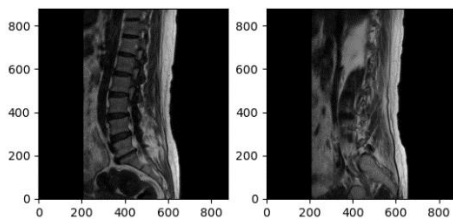


Fig. 6: Preprocessing of the image

Figure 6 shows the preprocessing step involved in the image in which a set of low level linear filter is used to denoised the 2D image. The preprocessing of the 2D image is carried out using Quadruplicate Up Sampling Operation. Thus the Denoised 2d images are up sampled two times therefore the proper image is selected for the labelling using the sagittal block matching thus the image get labelled down.

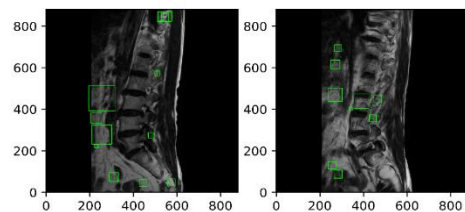


Fig. 7: Mapping the location edges and shape

Figure 7 depicts the elastic atlas mapping combined in a three-phase Atrous Net. The sub picture pairings are mapped in the registry as spatial information using this 3 phase Atrous Net, which includes the positions, edges, and shapes of the ROI image structures that are defined to produce binary disc templates.

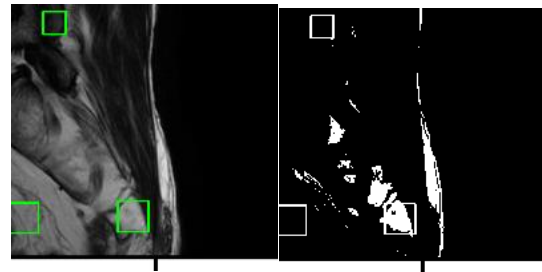


Fig. 8: Segmentation of the diseased area

Figure 8 shows the segmentation in the diseased area in the image the segmentation done by using atrous convolution that also extracts multiscale features in both cascade and parallel manner. Then the extracted feature pools are in large number, hence to select the optimal feature pool, the optimization is used that select best feature based on cobb angle, intensity, height and density.

4.4 Performance metrics of the proposed system

The performance of the proposed approach and the achieved outcome were explained in detail in this section which will depicts its efficiency in the accuracy, precision, recall and F1 score of the proposed system.

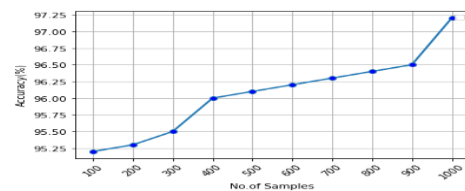


Fig. 9: Accuracy of the proposed model

The accuracy of the proposed model by the feature extraction and for prediction of the disease accuracy is given by figure 9 in which the scoliosis disease predicted with greater accuracy of about 97.25 percentage which is the high rate of accuracy for the prediction of disease. The accuracy of the proposed model is increased by using the 3DSpMRINet method uses the sparse learning for the prediction with high accuracy.

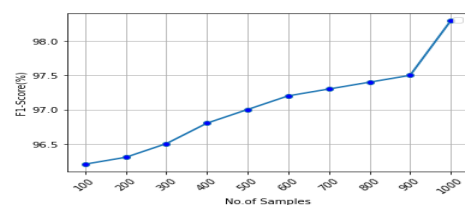


Fig. 10: F1 score of the proposed model

Figure 10 depicts the F1 score of the proposed model in which by calculating the harmonic mean of a classifier's output, the F1-score combines its precision and recall into a single metric the proposed model has the high F1 score value of about 99% with the 1000 number of samples as the rate of number the sample increases the F1 score of the proposed also get increases these shows the greater

efficiency of the proposed mode which is due to the feature selection by the 3 phase atrous net model.

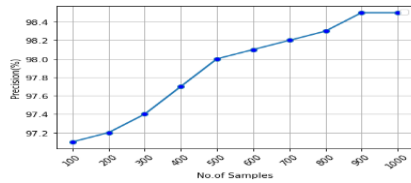


Fig. 11: Precision of the disease prediction

The exact and accurate being of the model is given by the precision thus the precision of the proposed model is depicted in figure 11 which shows the high precision of the proposed model as the number of the sample increases by 1000, the rate of precision is found to be 99% which is the high precision rate that give the accurate and exact being of the proposed model. The high precision rate is achieved by the 3DSpMRINet model which enhances the high rate of precision by using the elastic atlas mapping and segmentation.

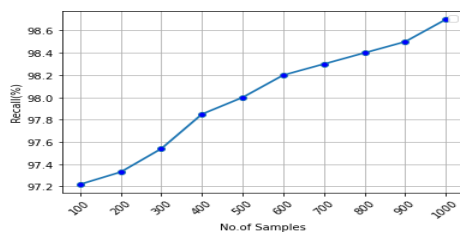


Fig. 12: Recall of the proposed model

Figure 12 shows the proposed models recall rate the higher the recall rate means the sensitive output prediction the proposed has the high recall rate with the increasing value of number of samples thus the recall rate of the proposed is about 99% thus the high recall rate is obtained for the proposed model. The higher recall rate of the proposed is achieved by the quadruple up sampling operation due to the double up sampling and the recall rate of the proposed increases with certain of higher extent.

4.5 Comparison results of the proposed method

This section highlights the proposed model performance by comparing it to the outcomes of existing approaches [35,36] and showing their results based on various metrics.

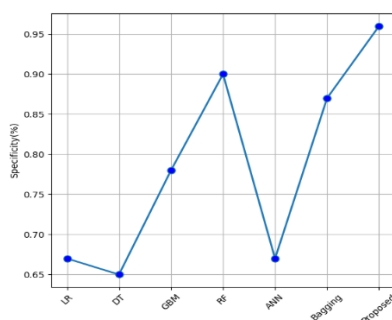


Fig. 13: Comparison of specificity with various model

Figure 13 depicts the specificity comparison of various model such as LR, DT, GBM, RF, ANN and Bagging. It is observed that the proposed scoliosis disease prediction model has the higher specificity of about 0.97 % which is the higher rate of specificity compared to the other existing models in which the LR has the specificity rate of about 0.67%, DT has the specificity rate of about 0.65% which is very low compared to the other models, GBM has the specificity rate of about 0.78%, RF has of specificity about 0.90%, ANN has the specificity of about 0.66% and bagging has the specificity of about 0.86%.

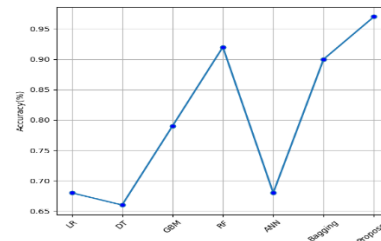


Fig. 14: Comparison of accuracy with various model

Figure 14 shows the accuracy comparison of the proposed model with the various existing model such as LR, DT, GBM, RF, ANN and Bagging. The accuracy of the scoliosis prediction model is greater than the other existing models which is about 0.97% for the proposed model thus the accuracy of the proposed is higher than the other existing model depicts the efficiency of the proposed model for prediction. Thus the accuracy of the existing models is given by the LR model has the accuracy in the rate of about 0.67%, DT has the accuracy rate of about 0.66% which is very low compared to the other existing model, GBM has the accuracy rate of about 0.79%, RF has the accuracy rate of 0.92%, ANN has the accuracy rate of 0.68%, and bagging has the accuracy rate of about 0.90%.

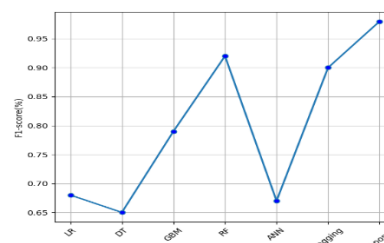


Fig. 15: Comparison of F1 Score of the proposed model with various existing model

Figure 15 exhibit the F1 score comparison with various existing model thus the proposed model has the larger F1 score ratio compared to the other existing models the ANN has the lowest F1 score of about 0.65% and RF has the score rate of about 0.93% compared to this the proposed model has the higher score rate of about 0.98%. The existing models such as LR has the F1 score of 0.68%, GBM has the F1 score rate of about 0.79% and bagging model has the F1 score rate of about 0.90%.

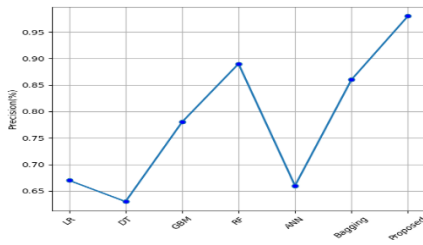


Fig. 16: Comparison of precision with various model

The precision of the proposed model is compared with various existing model is illustrated in figure 16 shows the precision rate of the disease prediction model is higher in the range of about 0.99% which is the highest range of precision compared to other existing model. The existing model such as LR, DT, GBM, RF, ANN and bagging has the precision in the rate of about 0.67%, 0.63%, 0.78%, 0.89%, 0.66% and 0.86% respectively.

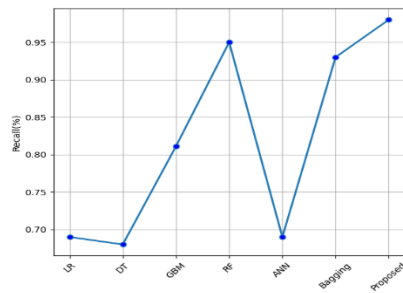


Fig. 17: Comparison of recall with various model

Figure 17 shows the recall rate of the scoliosis disease prediction model compared to the other existing models the recall rate of the proposed is found to be 0.99% which is higher rate of recall compared to other existing models. The existing models such as LR, DF, GBM, RF, ANN and bagging has the recall rate of 0.68%, 0.67%, 0.81%, 0.95%, 0.69% and 0.94% respectively.

Overall, the scoliosis disease prediction with the specificity, accuracy, F1 Score, precision and recall rate shows the efficiency of the proposed model for its disease prediction that incorporate with the Segmentation accuracy and classification accuracy have increased by using three phases of segmentation, sub sampling, feature selection, and sparse learning. Thus the result achieved is given by 0.97% of specificity, 0.97% of accuracy, 0.98% of F1 score, 0.99% of precision and 0.99% of recall rate respectively.

5. Conclusion

Effective Scoliosis disease prediction using Quadruple up sampling, 3 phase atrous net and 3DSpMRINet based on preprocessing, labelling and segmentation has been proposed in this research to solve the issue in predicting degree of severity in image, unpredictable predefined plane

image, over segmentation problem, distortion, inconsistency, less detail on disease, low quality image and low accuracy disease prediction. The segmentation and the elastic atlas mapping together form the 3 phase atrous net which increases the quality and provide the sub image pair mapped in the ROI image. The 3DSpMRINet provide the sparse learning for the disease prediction in the feature weight vector thus they provide the high accuracy of 98% in the prediction of the scoliosis disease. The degree of severity is predictable using the quadruple up sampling operation, distortion and inconsistency is solved by 3 phase atrous net and quality of the prediction is increased by 3DSpMRINet model thus segmentation and mapping of the diseased area is easier so that it is easy to predict the disease area with high accuracy of about 0.98%, precision of about 0.99% and recall rate of about 0.99%. By utilizing the proposed methodology in the scoliosis disease prediction the proposed model achieves high accuracy and quality of the disease prediction with better F1 score and precision.

References

- [1] R. Kritschil, M. Scott, G. Sowa, and N. Vo, "Role of autophagy in intervertebral disc degeneration," *Journal of cellular physiology*, vol. 237, no. 2, pp.1266-1284, 2022.
- [2] D. Sakai, J. Schol and M. Watanabe, "Clinical Development of Regenerative Medicine Targeted for Intervertebral Disc Disease," *Medicina*, vol. 58, no. 2, pp. 267, 2022.
- [3] G. Bjornsdottir, L. Stefansdottir, G. Thorleifsson, P. Sulem, K. Norland, E. Ferkingstad, A. Oddsson, F. Zink, S.H. Lund, M.S. Nawaz and G. Bragi Walters, "Rare SLC13A1 variants associate with intervertebral disc disorder highlighting role of sulfate in disc pathology," *Nature communications*, vol. 13, no. 1, pp.1-13, 2022.
- [4] T.J. DiStefano, K. Vaso, G. Danias, H.N. Chionuma, J.R. Weiser and J.C. Iatridis, "Extracellular vesicles as an emerging treatment option for intervertebral disc degeneration: therapeutic potential, translational pathways, and regulatory considerations," *Advanced Healthcare Materials*, vol. 11, no. 5, pp. 2100596, 2022.
- [5] J. Zieba, K.N. Forlenza, K. Heard, J.H. Martin, M. Bosakova, D.H. Cohn, S.P. Robertson, P. Krejci, and D. Krakow, "Intervertebral disc degeneration is rescued by TGFβ/BMP signaling modulation in an ex vivo filamin B mouse model," *Bone Research*, vol. 10, no. 1, pp.1-12, 2022.
- [6] S. Chen, L. Lei, Z. Li, F. Chen, Y. Huang, G. Jiang, X. Guo, Z. Zhao, H. Liu, H. Wang and C. Liu, "Grem1 accelerates nucleus pulposus cell apoptosis and intervertebral disc degeneration by inhibiting TGF-β-mediated Smad2/3 phosphorylation," *Experimental & Molecular Medicine*, pp.1-13, 2022.
- [7] M. Yang, D. Xiang, Y. Chen, Y. Cui, S. Wang, and W. Liu, "An Artificial PVA-BC Composite That Mimics the Biomechanical Properties and Structure of a Natural Intervertebral Disc," *Materials*, vol. 15, no. 4, pp.1481, 2022.
- [8] Z. Wang, H. Chen, Q. Tan, J. Huang, S. Zhou, F. Luo, D. Zhang, J. Yang, C. Li, B. Chen, and X. Sun, "Inhibition of

- aberrant Hif1 α activation delays intervertebral disc degeneration in adult mice,” *Bone Research*, vol. 10, no. 1, pp.1-16, 2022.
- [9] C. Wang, S. Guo, Q. Gu, X. Wang, L. Long, C. Xiao, M. Xie, H. Shen and S. Li, “Exosomes: A promising therapeutic strategy for intervertebral disc degeneration,” *Experimental Gerontology*, pp.111806, 2022.
- [10] T. Ohnishi, N. Iwasaki, and H. Sudo, “Causes of and Molecular Targets for the Treatment of Intervertebral Disc Degeneration: A Review,” *Cells*, vol. 11, no. 3, pp. 394, 2022.
- [11] X. Bai, M. Jiang, J. Wang, S. Yang, Z. Liu, H. Zhang, and X. Zhu, “Cyanidin attenuates the apoptosis of rat nucleus pulposus cells and the degeneration of intervertebral disc via the JAK2/STAT3 signal pathway in vitro and in vivo,” *Pharmaceutical Biology*, vol. 60, no. 1, pp.427-436, 2022.
- [12] Y. Fan, L. Zhao, Y. Lai, K. Lu, and J. Huang, “CRISPR/Cas9-Mediated Loss-of-Function of β -Catenin Attenuates Intervertebral Disc Degeneration,” *Molecular Therapy-Nucleic Acids*, 2022.
- [13] V. Francisco, J. Pino, M.Á. González-Gay, F. Lago, J. Karppinen, O. Tervonen, A. Mobasheri, and O. Gualillo, “A new immunometabolic perspective of intervertebral disc degeneration,” *Nature Reviews Rheumatology*, vol. 18, no. 1, pp.47-60, 2022.
- [14] T. Wu, X. Jia, Z. Zhu, K. Guo, Q. Wang, Z. Gao, X. Li, Y. Huang, and D. Wu, “Inhibition of miR-130b-3p restores autophagy and attenuates intervertebral disc degeneration through mediating ATG14 and PRKAA1,” *Apoptosis*, pp.1-17, 2022.
- [15] F. Mahyudin, C.R.S. Prakoeswa, H.B. Notobroto, D. Tinduh, R. Ausrin, F.A. Rantam, H. Suroto, D.N. Utomo, and S. Rhatomy, “An update of current therapeutic approach for Intervertebral Disc Degeneration: A review article,” *Annals of Medicine and Surgery*, pp.103619, 2022.
- [16] K. Miyazaki, S. Miyazaki, T. Yurube, Y. Takeoka, Y. Kanda, Z. Zhang, Y. Kakiuchi, R. Tsujimoto, H. Ohnishi, T. Matsuo, and M. Ryu, “Protective Effects of Growth Differentiation Factor-6 on the Intervertebral Disc: An In Vitro and In Vivo Study,” *Cells*, vol. 11, no. 7, pp.1174, 2022.
- [17] K. Yamada, N. Iwasaki, and H. Sudo, “Biomaterials and Cell-Based Regenerative Therapies for Intervertebral Disc Degeneration with a Focus on Biological and Biomechanical Functional Repair: Targeting Treatments for Disc Herniation,” *Cells*, vol. 11, no. 4, pp. 602, 2022.
- [18] M.P. Culbert, J.P. Warren, A.R. Dixon, H.L. Fermor, P.A. Beales, and R.K. Wilcox, “Evaluation of injectable nucleus augmentation materials for the treatment of intervertebral disc degeneration,” *Biomaterials Science*, 2022.
- [19] S. Khalid, S. Ekram, A. Salim, G.R. Chaudhry, and I. Khan, “Transcription regulators differentiate mesenchymal stem cells into chondroprogenitors, and their in vivo implantation regenerated the intervertebral disc degeneration,” *World Journal of Stem Cells*, vol. 14, no. 2, pp.163, 2022.
- [20] H. Liang, R. Luo, G. Li, W. Zhang, Y. Song, and C. Yang, “The Proteolysis of ECM in Intervertebral Disc Degeneration,” *International Journal of Molecular Sciences*, vol. 23, no. 3, pp.1715, 2022.
- [21] C. Wang, L. Cui, Q. Gu, S. Guo, B. Zhu, X. Liu, Y. Li, X. Liu, D. Wang, and S. Li, “The Mechanism and Function of miRNA in Intervertebral Disc Degeneration,” *Orthopaedic Surgery*, vol. 14, no. 3, pp.463-471, 2022.
- [22] Y. Wang, J. Kang, X. Guo, D. Zhu, M. Liu, L. Yang, G. Zhang, and X. Kang, “Intervertebral disc degeneration models for pathophysiology and regenerative therapy-benefits and limitations,” *Journal of Investigative Surgery*, vol. 35, no. 4, pp.935-952, 2022.
- [23] S. Ashwinkumar, S. Rajagopal, V. Manimaran, and B. Jegajothi, “Automated plant leaf disease detection and classification using optimal MobileNet based convolutional neural networks,” *Materials Today: Proceedings*, vol. 51, pp.480-487, 2022.
- [24] S. Shastri, I. Kansal, S. Kumar, K. Singh, R. Popli, and V. Mansotra, “CheXImageNet: a novel architecture for accurate classification of Covid-19 with chest x-ray digital images using deep convolutional neural networks,” *Health and Technology*, pp.1-12, 2022.
- [25] F. Rehman, S.I.A. Shah, N. Riaz, and S.O. Gilani, “A robust scheme of vertebrae segmentation for medical diagnosis,” *IEEE Access*, vol. 7, pp.120387-120398, 2019.
- [26] E.J. Hwang, S. Kim, and J.Y. Jung, “Bone Marrow Radiomics of T1-Weighted Lumbar Spinal MRI to Identify Diffuse Hematologic Marrow Diseases: Comparison With Human Readings,” *IEEE Access*, vol. 8, pp.133321-133329, 2020.
- [27] F. Fallah, S.S. Walter, F. Bamberg, and B. Yang, “Simultaneous volumetric segmentation of vertebral bodies and intervertebral discs on fat-water MR images,” *IEEE journal of biomedical and health informatics*, vol. 23, no. 4, pp.1692-1701, 2018.
- [28] L. Lin, X. Tao, W. Yang, S. Pang, Z. Su, H. Lu, S. Li, Q. Feng, and B. Chen, “Quantifying Axial Spine Images Using Object-Specific Bi-Path Network,” *IEEE Journal of Biomedical and Health Informatics*, vol. 25, no. 8, pp.2978-2987, 2021.
- [29] S. Pang, C. Pang, L. Zhao, Y. Chen, Z. Su, Y. Zhou, M. Huang, W. Yang, H. Lu, and Q. Feng, “Spineparsenet: spine parsing for volumetric MR image by a two-stage segmentation framework with semantic image representation,” *IEEE Transactions on Medical Imaging*, vol. 40, no. 1, pp.262-273, 2020.
- [30] X. Li, Q. Dou, H. Chen, C.W. Fu, X. Qi, D.L. Belavý, G. Armbrecht, D. Felsenberg, G. Zheng, and P.A. Heng, “3D multi-scale FCN with random modality voxel dropout learning for intervertebral disc localization and segmentation from multi-modality MR images,” *Medical image analysis*, vol. 45, pp.41-54, 2018.
- [31] H. Wang, T. Zhang, K.M.C. Cheung, and G.K.H. Shea, “Application of deep learning upon spinal radiographs to predict progression in adolescent idiopathic scoliosis at first clinic visit,” *EclinicalMedicine*, vol. 42, pp.101220, 2021.
- [32] M.L. Nault, M. Beauséjour, M. Roy-Beaudry, J.M. Mac-Thiong, J. de Guise, H. Labelle, and S. Parent, “A predictive model of progression for adolescent idiopathic scoliosis based on 3D spine parameters at first visit,” *Spine*, vol. 45, no. 9, pp.605-611, 2020.
- [33] J. Zhang, K.Y. Cheuk, L. Xu, Y. Wang, Z. Feng, T. Sit, K.L. Cheng, E. Nepotchaykh, T.P. Lam, Z. Liu, and A.L. Hung, “A validated composite model to predict risk of curve progression in adolescent idiopathic scoliosis,” *EclinicalMedicine*, vol. 18, p.100236, 2020.

- [34] J. Yi, P. Wu, Q. Huang, H. Qu, and D.N. Metaxas, "Vertebra-focused landmark detection for scoliosis assessment," *In 2020 IEEE 17th International Symposium on Biomedical Imaging (ISBI). IEEE*, pp. 736-740, 2020, April.
- [35] J. Bradley, and S. Rajendran, "Developing predictive models for early detection of intervertebral disc degeneration risk," *Healthcare Analytics*, vol. 2, pp. 100054, 2022.
- [36] S. Ma, Y. Huang, X. Che, and R. Gu, "Faster RCNN-based detection of cervical spinal cord injury and disc degeneration," *Journal of Applied Clinical Medical Physics*, vol. 21, no. 9, pp.235-243, 2020.